

FIG. 1A

FIG. 1B

2001年9月20日 11時29分

No. 1613 P. 46

INDUCTANCE DEVICE DRIVING SYSTEM . . .
Nishida et al.
Greer, Burns & Crain, Ltd. (Patrick Burns)
Ref. No. 0941.65858
Sheet 2 of 16 (312) 360 0080

2001年 9月20日 11時29分

INDUCTANCE DEVICE DRIVING SYSTEM . . .
Nishida et al.
Greer, Burns & Crain, Ltd. (Patrick Burns)
Ref. No. 0941.65858
Sheet 3 of 16 (312) 360 0080

No. 1613 P. 41

FIG. 3A

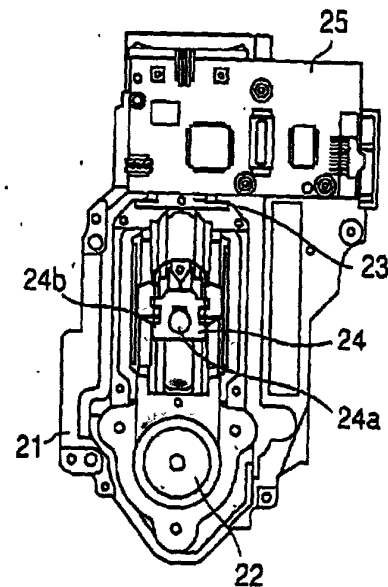


FIG. 3B

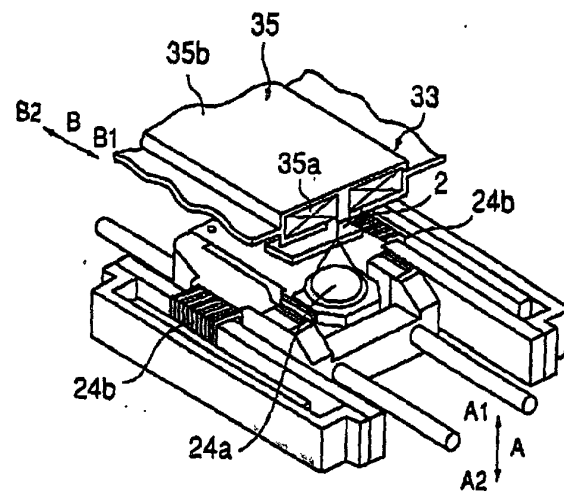


FIG. 3C

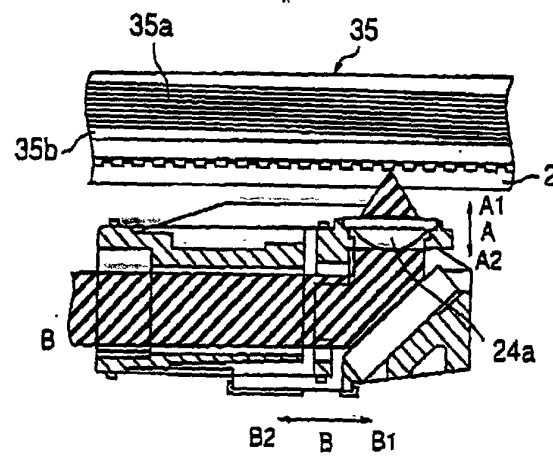


FIG.4

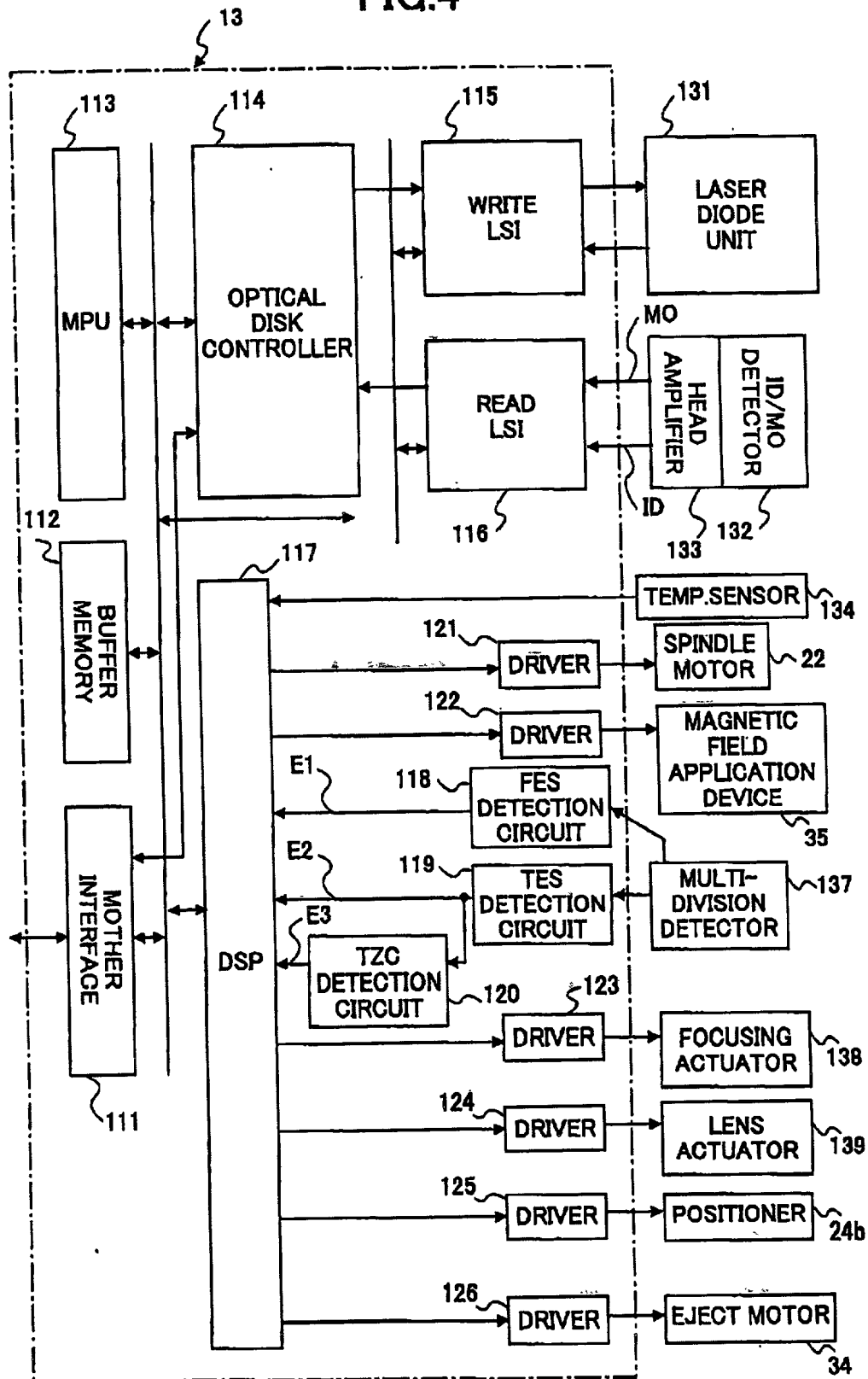


FIG. 5

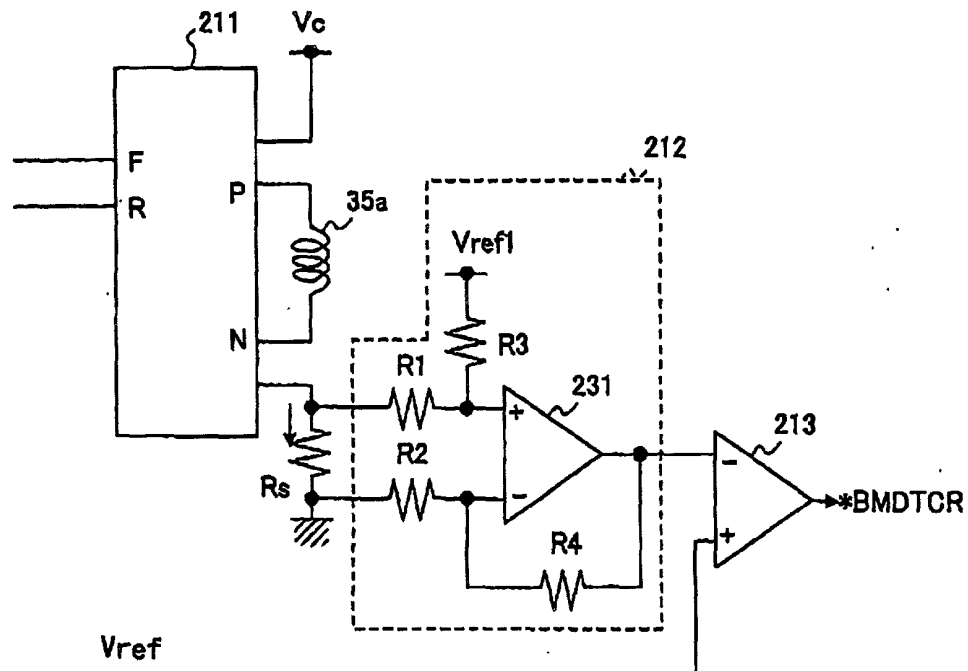
210

FIG. 6

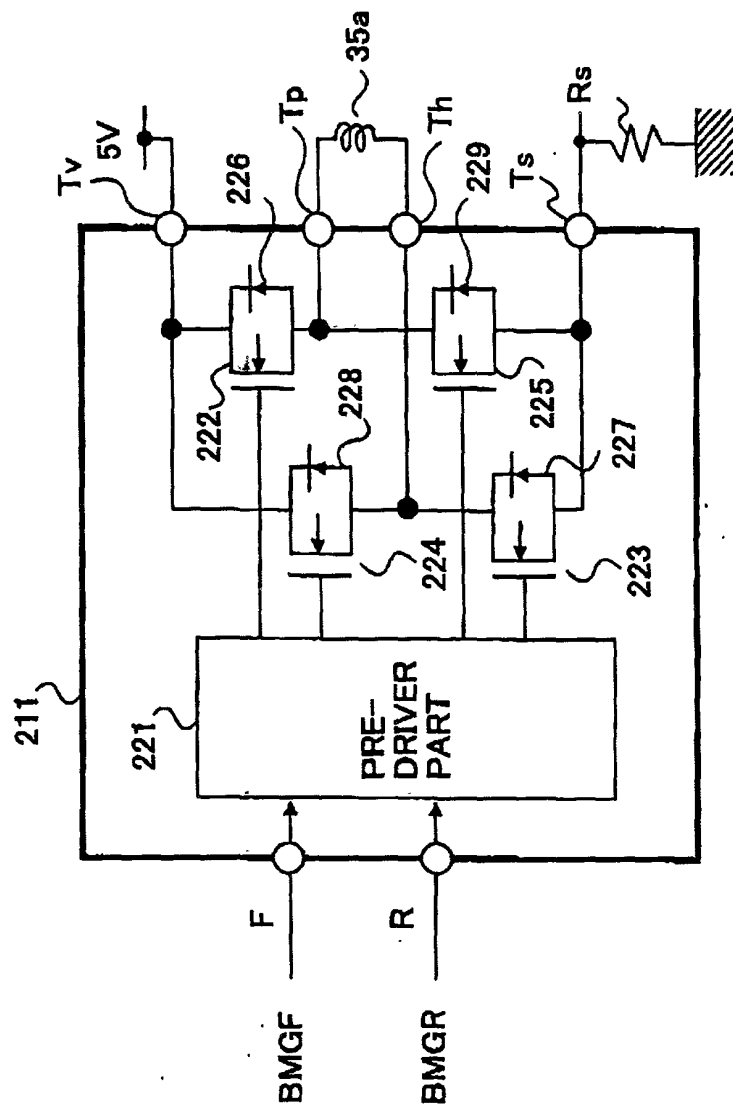


FIG. 7

BMGF	BMGR	P OUTPUT	N OUTPUT	NOTE
H	L	H	L	POSITIVE CHANGE(P→N)
L	H	L	H	NEGATIVE CHANGE(N→P)
L	L	L	L	SHORT BREAK

FIG.8

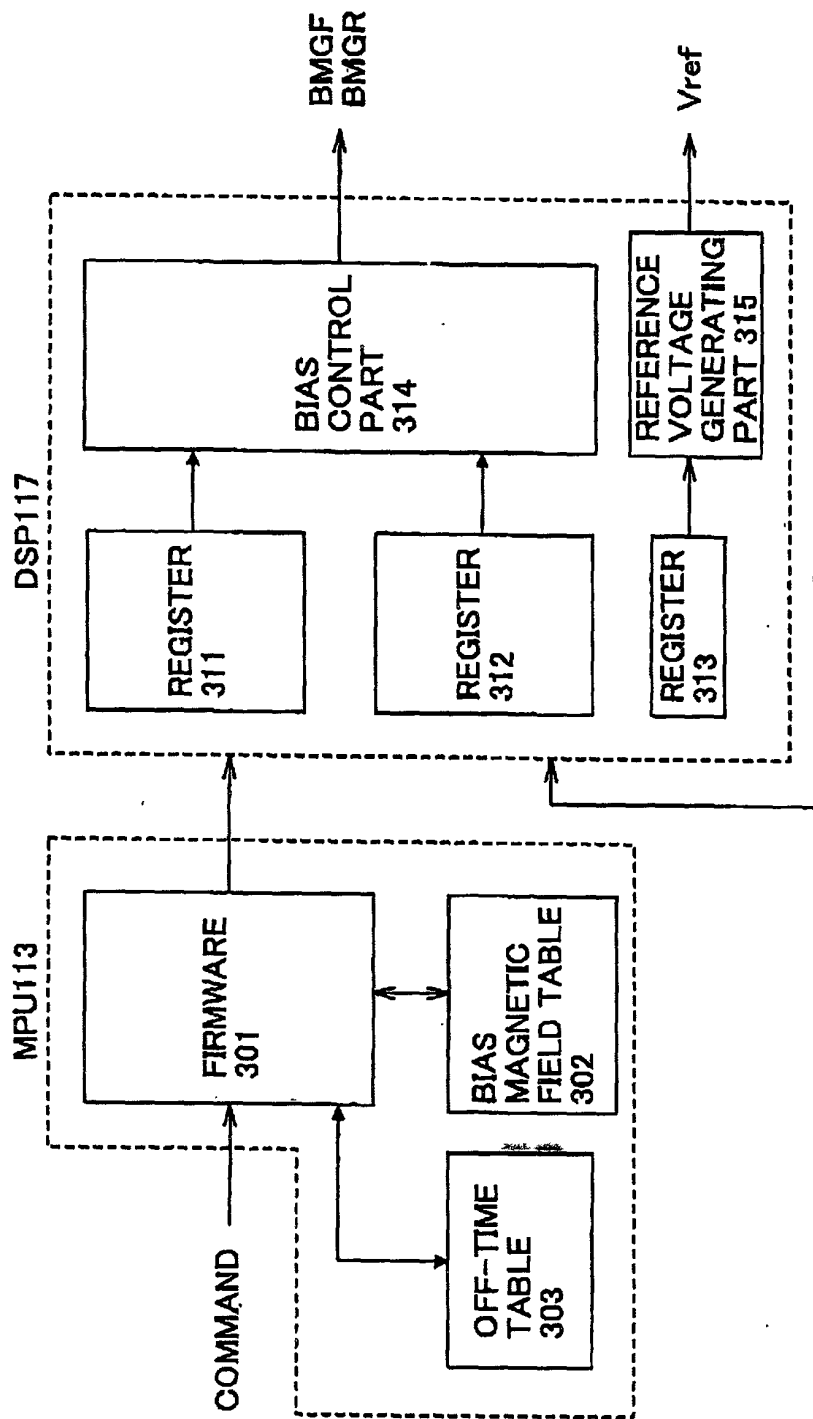


FIG.9

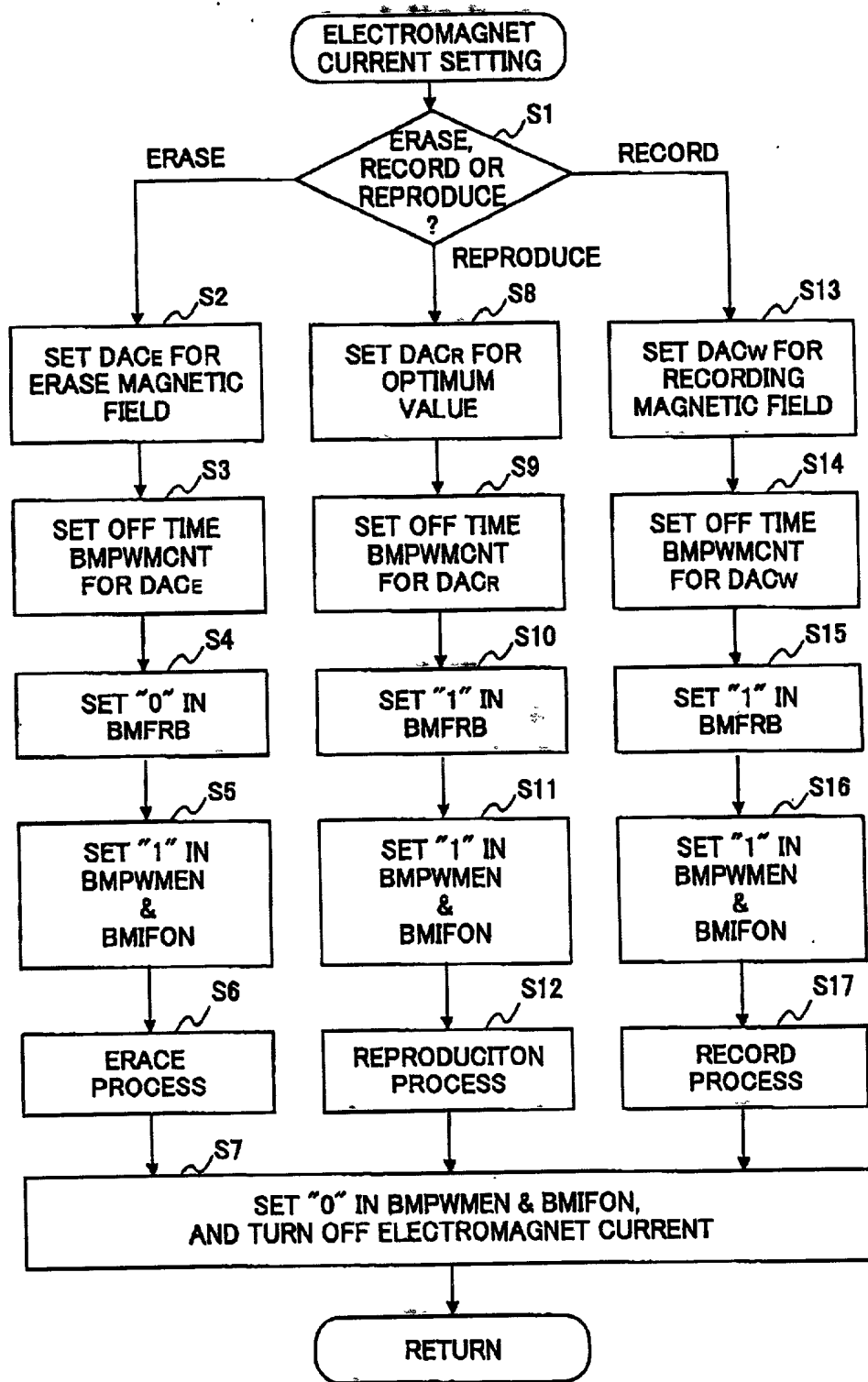


FIG.10A

ZONE NUMBER	ELECTROMAGNET ELECTRIC CURRENT			
	ERASE	RECORD	INITIAL VALUE FOR REPRODUCTION	CALIBRATION COEFFICIENT
Z1	$I_E[\text{mA}] (\text{DACE})$	$I_W[\text{mA}] (\text{DACW})$	$I_{RZ1}[\text{mA}] (\text{DACR}_{Z1})$	α_1
Z2			$I_{RZ2}[\text{mA}] (\text{DACR}_{Z2})$	α_2
Z3			$I_{RZ3}[\text{mA}] (\text{DACR}_{Z3})$	α_3
Z4			$I_{RZ4}[\text{mA}] (\text{DACR}_{Z4})$	α_4
Z5			$I_{RZ5}[\text{mA}] (\text{DACR}_{Z5})$	α_5
Z6			$I_{RZ6}[\text{mA}] (\text{DACR}_{Z6})$	α_6
Z7			$I_{RZ7}[\text{mA}] (\text{DACR}_{Z7})$	α_7
Z8			$I_{RZ8}[\text{mA}] (\text{DACR}_{Z8})$	α_8
Z9			$I_{RZ9}[\text{mA}] (\text{DACR}_{Z9})$	α_9
Z10			$I_{RZ10}[\text{mA}] (\text{DACR}_{Z10})$	α_{10}
Z11			$I_{RZ11}[\text{mA}] (\text{DACR}_{Z11})$	α_{11}

FIG.10B

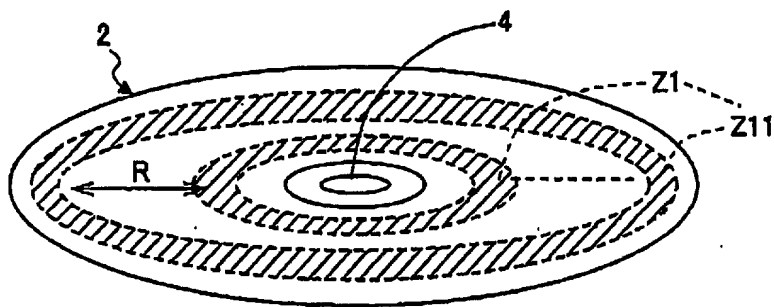
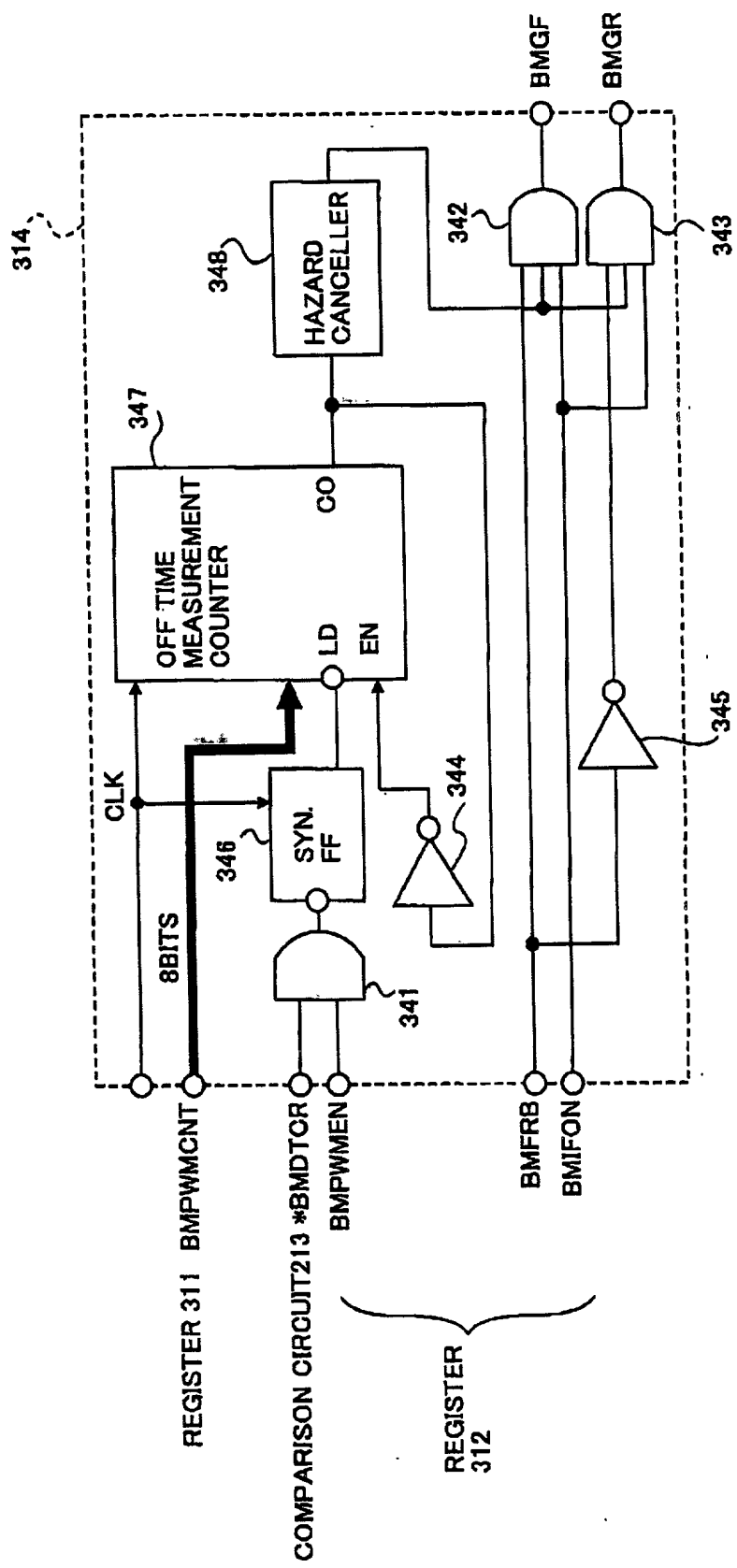


FIG. 11

303

BLAS_DAC	BMPWMCNT
0x00~0x0f	0x18
0x10~0x1f	0x10
0x20~0x3f	0x08
0x40~0x7f	0x04
0x80~0xff	0x01

FIG.12



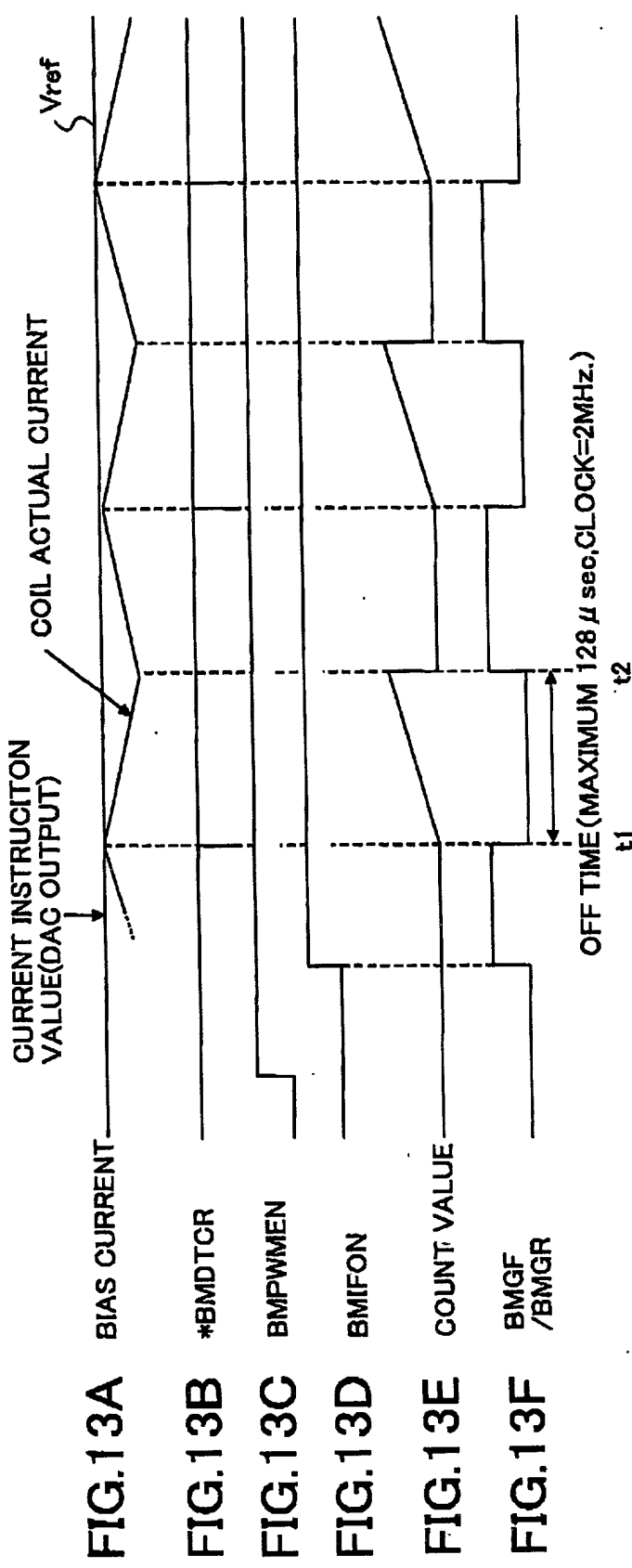


FIG. 14

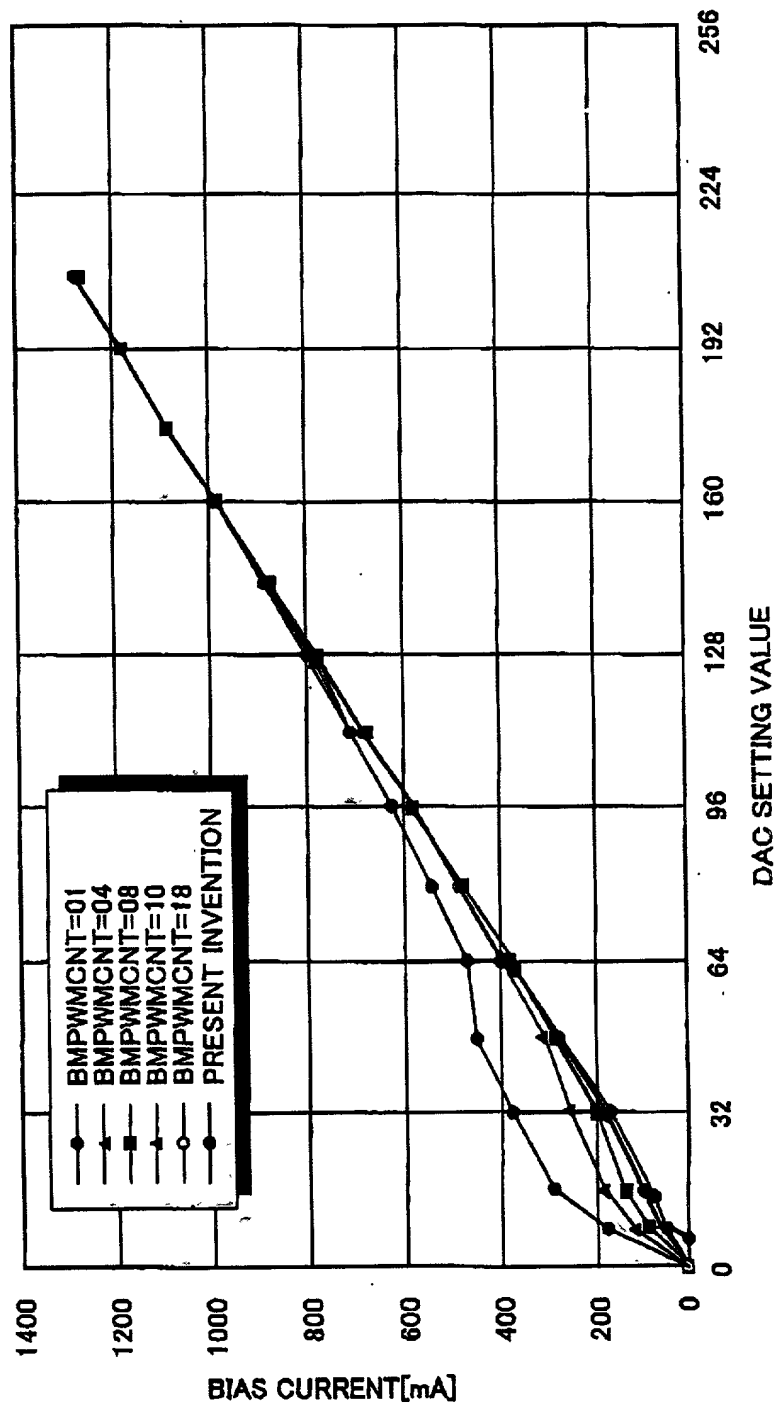


FIG.15

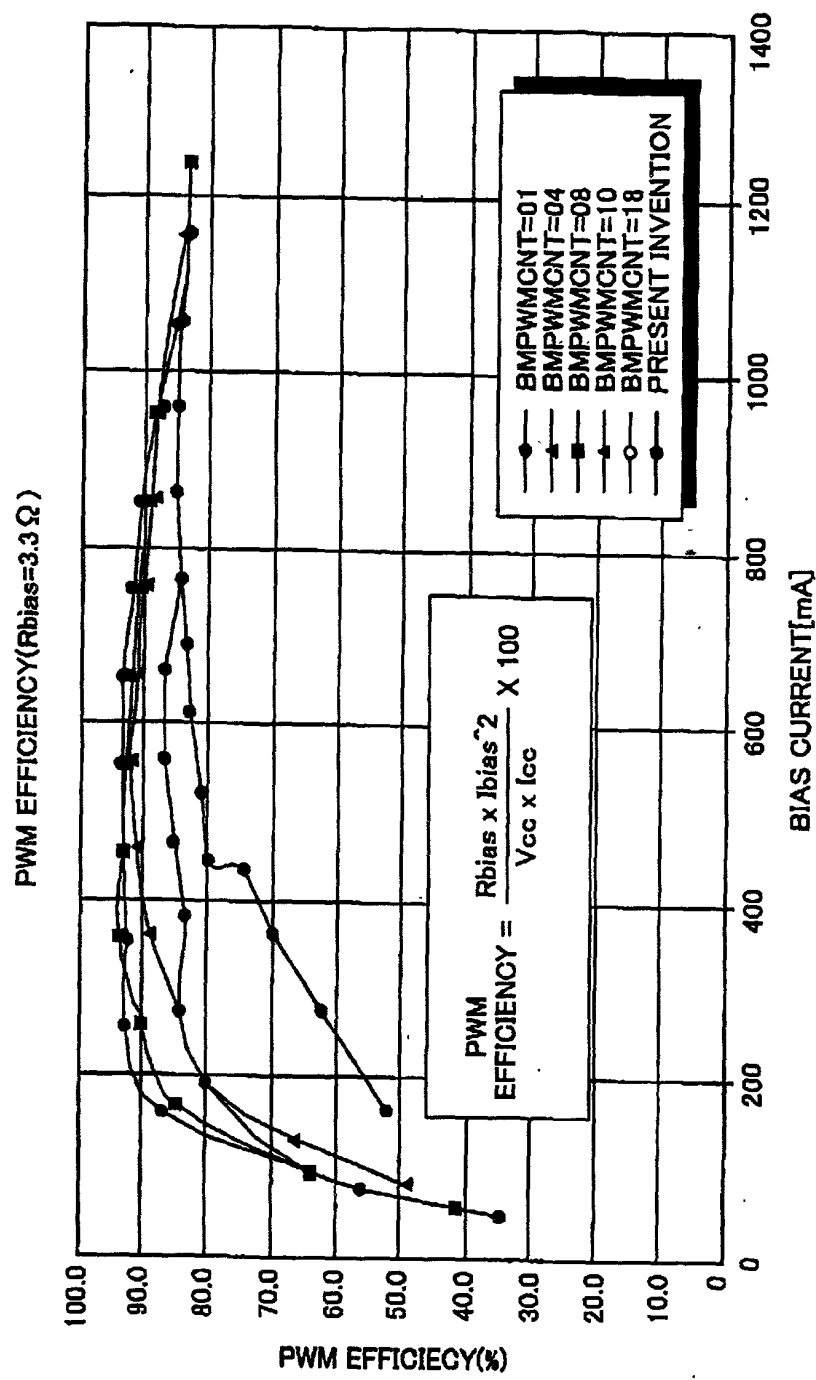


FIG.16

